Short-range magnetic order in holmium-praseodymium superlattices

1995 J. Phys.: Condens. Matter 7 L417

(http://iopscience.iop.org/0953-8984/7/31/002)

J. Phys.: Condens. Matter 7 (1995) L417–L423. Printed in the UK

LETTER TO THE EDITOR

Short-range magnetic order in holmium–praseodymium superlattices

J A Simpson†, D F McMorrow‡, R A Cowley†, R C C Ward† and M R Wells†

† Oxford Physics, Clarendon Laboratory, Parks Road, Oxford OX1 3PU, UK
‡ Department of Solid State Physics, Risø National Laboratory, DK 4000 Roskilde, Denmark

Received 20 May 1995

Abstract. The chemical and magnetic structures of Ho/Pr superlattices have been studied by a combination of x-ray and neutron scattering techniques. While the Ho blocks are hcp, the Pr blocks retain their bulk-like dhcp structure, but with a stacking of the hexagonal atomic planes that is not coherent between successive blocks. Below a Néel temperature of ~110 K, the Ho magnetic moments order into a basal plane spiral with a magnetic coherence length that is limited to the width of a single Ho block, even for a sample comprising of only six atomic planes of Pr. These observations are discussed in terms of the differing band structures of the two elements.

Metallic superlattices grown by molecular beam epitaxy (MBE) display a wealth of magnetic properties not exhibited by the bulk state that are challenging our understanding of magnetic interactions. In the case of the rare earths, attention has focused largely on combining a magnetic heavy rare earth element with a non-magnetic spacer such as Y or Lu [1]. For systems of this type, long-range magnetic order propagates through the spacer layers with coherence extending over many superlattice repeats [2]. Rare-earth superlattices also exhibit novel magnetic structures, such as the transition of Ho to a ferromagnet at low temperatures in Ho/Lu [3]. Whereas heavy rare earth elements, Er, Ho, etc, form magnetic structures that are modulated along the c direction, the light rare earths are modulated in the basal plane with interactions along c mainly restricted to nearest neighbours only. To date, little is known about superlattices with mixed heavy/light rare earth combinations, and to our knowledge the study of Nd/Y [4] is the only one yet reported. (Although Y is not a rare earth element, it may be regarded as one due to its similar electronic and structural properties.) In this letter we present the results of a study of Ho/Pr superlattices, where both elements are magnetic, but have different crystal structures and magnetic properties. Our results are compared with those of the Nd/Y system.

Ho has the hcp crystal structure, and below an ordering temperature of 132.2 K the magnetic moments are confined to the basal plane. While ferromagnetically coupled within each basal plane, the orientation of the moments in successive basal planes along the c axis rotates through an angle, as first determined by Koehler and coworkers [5]. This helical arrangement is characterized by a wavevector q, and at the onset of ordering $q \approx 0.275c^*$. The wavevector reduces smoothly on cooling until below ≈30 K the wavevector locks into a series of commensurable values [6] which are accounted for by the spin slip model [7, 8]. Below 20 K the moments tilt out of the basal plane due to dipolar interactions, and the wavevector locks into $(\frac{1}{6})c^*$. In contrast, Pr has the dhcp structure and the crystallographic

0953-8984/95/310417+07$19.50

sites in the unit cell may be divided into those having hexagonal symmetry and those with an approximately cubic environment. Pr is a non-Kramers ion, and the ground state crystal field levels for both of these sites are singlets [9]; other multiplet states are significantly higher in energy [10] and below ~40 K only the singlet state is occupied. Magnetic ordering occurs through the hyperfine interaction [11, 12], with long-range order developing below 45 mK [13, 14], and takes the form of a longitudinal wave along the *b* axis. A summary of the magnetic properties of Pr is given by Jensen and Mackintosh [15].

The Ho/Pr superlattices were prepared by MBE using the growth techniques previously described by McMorrow *et al* [16]. A buffer layer of Nb was first grown on a sapphire substrate, with the $[11\bar{2}0]$ direction normal to the surface, at a substrate temperature of 1000 °C. A seed layer of ≈1000 Å of Y, with the growth direction along *c*, was then deposited. The optimum substrate temperature for MBE growth of metallic superlattices was found by Flynn to be $\sim 3T_m/8$ for an element with melting point T_m [17]. This represents a compromise between trying to limit the interdiffusion that occurs at elevated temperatures, while maintaining sufficient surface mobility to prevent island growth as the temperature is reduced. For systems consisting of two heavy rare earth elements with similar melting points, the superlattices have been grown at a temperature of 400 °C. Pr has a significantly lower melting point than Ho; consequently the growth temperature of this system was reduced to 350 °C. Three samples were prepared with nominal block sizes Ho_{20}/Pr_{20}, Ho_{30}/Pr_{10}, and Ho_{24}/Pr_6, where the subscripts refer to the number of atomic planes in each block, and each biblock unit was repeated 80 times. The growth was monitored by *in situ* RHEED patterns which indicated uniform two-dimensional growth for the Y seed and the first Pr layer. During subsequent growth the crystallographic quality of successive blocks deteriorated, probably due to the lattice mismatch and the different crystal structures preferred by Ho and Pr. This was not observed in the heavy rare earth superlattices, where the RHEED patterns remained essentially unchanged throughout the growth process. We have investigated the consequences of this deterioration with our x-ray and neutron scattering measurements.

The neutron scattering measurements were carried out using the triple-axis spectrometers TAS1 and TAS6 at the DR3 reactor of Risø National Laboratory, Denmark. The collimation from reactor to detector was selected to give a wavevector resolution of approximately 0.01 $Å^{-1}$ for 5meV incident neutrons. Contamination from higher-order neutrons was reduced by the use of a cooled Be filter. The samples were mounted with the $(h0\ell)$ crystallographic plane in the scattering plane and cooled using a variable temperature cryostat. Measurements were made with the wavevector transfer, Q, along the $[00\ell]$ and $[10\ell]$ reciprocal lattice directions at a range of temperatures. The crystalline quality of the samples was also investigated using a triple-crystal x-ray diffractometer, by performing scans with the wavevector transfer along $[00\ell]$ and transverse through the Bragg peaks.

Typical x-ray measurements for the Ho_{30}/Pr_{10} superlattice are shown in figure 1(a). This scan, with the wavevector transfer along $[00\ell]$, is sensitive only to the stacking sequence of the planes perpendicular to *c*, and reveals a series of relatively sharp peaks with separations in Q of $2\pi/L$ ($Å^{-1}$), which indicates the superlattice has coherent growth along this direction. From the width of these peaks, the structural coherence length is found to be ≈250 Å. (The real space coherence length, ξ, was calculated from the FWHM in reciprocal space, ΔQ, using $\xi = 2\pi/\Delta Q$ and neglecting the very high resolution of the x-ray diffractometer.) This value is somewhat smaller than found in previous studies of heavy rare earth superlattices; for example, the structural coherence length of the Ho/Y system was found to be ~ 2000 Å. A transverse scan through the (002) peak had a width of ≈1° (FWHM) for each sample, as shown in table 1. This is significantly larger than found for

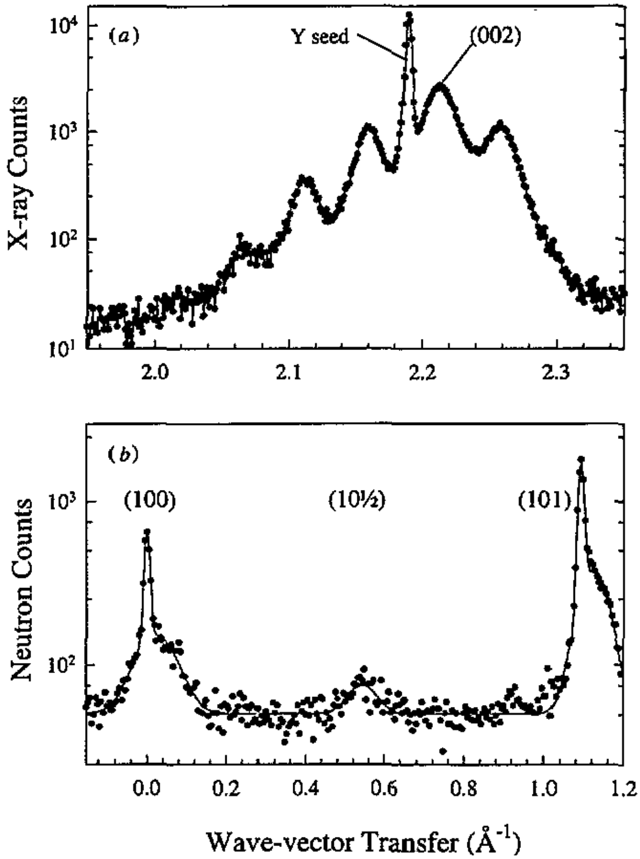

Figure 1. (a) The x-ray scattering of the Ho_{20}/Pr_{10} system taken with the wavevector transfer (using the hcp reciprocal lattice notation) along [00ℓ] around the (002) position. The solid line shows five Gaussian peaks of equal separations in Q, and the peak near $Q = 2.19$ Å^{-1} is due to the Y seed layer. In (b) the neutron scattering data from the Ho_{20}/Pr_{10} sample with Q along [10ℓ] show peaks at (100), (101) and also $(10\frac{1}{2})$. These have been modelled by three Gaussians, but unlike the [00ℓ] peaks these are much broader. The peaks at (100) and (101) have an additional, sharper component which is due to scattering from the Y substrate. The solid line is a fit to a constant background and a sum of these five Gaussians.

Table 1. Summary of properties determined by our x-ray and neutron scattering measurements.

Sample	Nominal Ho block length (Å)	X-ray rocking curve (FWHM) (°)	Magnetic coherence length (Å)	T_N (K)	q(10 K) (c*)	$q(T_N)$ (c*)
Ho_{20}/Pr_{20}	56	1.57±0.05	65(7)	112.5 ± 0.5	0.230	0.271
Ho_{30}/Pr_{10}	84	1.26±0.05	91(9)	117.5 ± 0.5	0.224	0.270
Ho_{24}/Pr_{6}	67	1.36±0.05	84(8)	115.0 ± 0.5	0.232	0.277

the Ho/Y system, where the typical width was 0.2° (FWHM) [18], and is consistent with the deterioration of the RHEED pattern during growth.

The neutron scattering data of figure 1(b) shows the scattering from the Ho_{20}/Pr_{20} superlattice at room temperature when the wavevector transfer was varied along the [10ℓ] reciprocal lattice direction. Peaks are present at (100), (101) and ($10\frac{1}{2}$) (in the hcp reciprocal lattice notation). This measurement is sensitive to the orientation of the basal plane layers, and the presence of a peak at ($10\frac{1}{2}$) shows that some of the superlattice, presumably the Pr blocks, have their bulk like dhcp structure. All the peaks along [10ℓ] have a component which is much broader than the features observed along [00ℓ] in figure 1(a) (after allowing for the differences in instrument resolution), and also contain sharper features due to the Y seed and cap. The solid line in figure 1(b) is a fit to a constant background and five Gaussians: three broad peaks to represent the superlattice (100), ($10\frac{1}{2}$) and (101) reflections, and two sharper peaks to account for the scattering from the Y seed. The width of the broad peaks corresponds to a real-space correlation length of ≈85 Å for the superlattice. (This is obtained by firstly correcting the FWHM, ΔQ, for instrumental resolution and then following the same method as described above for calculating the coherence length along c.) This width corresponds to approximately one Ho or Pr block length, and shows that the stacking sequence of the hexagonal atomic planes is not ordered coherently for more than a single block. For example, if a Pr block adopts the ABAC sequence for stacking of the basal plane layers, the next Ho block may form either an ABAB or an ACAC stacking, but the choice of the stacking is unrelated to the previous Ho layer. Interfacial roughness will then distort the stacking of the planes, and could well be responsible for the much larger mosaic spread than found in heavy-rare-earth superlattices.

The neutron scattering observed from the Ho_{20}/Pr_{20} and Ho_{30}/Pr_{10} samples at 10 K is shown in figure 2. In addition to the features resulting from the nuclear scattering in figure 1, there are also magnetic peaks positioned at $+q$ and $-q$, indicating that the Ho magnetic moments order in a helical structure. The most striking feature of these peaks is that they are extremely broad, and unlike the nuclear scattering do not display any superlattice satellite structure. The magnetic coherence lengths derived from the widths of the broad peaks has a value that corresponds to one Ho block length in each case, as summarized in table 1. This shows that the phase and chirality of the Ho spiral is not transmitted coherently through the Pr blocks. This result is very different from that of previous studies of systems such as Dy/Y [2] and Ho/Y [18] where long-range coherent magnetic order is established across several bi-blocks of the non-magnetic spacer. Scans were also performed with Q along the [$h00$] direction, through both the nuclear and magnetic peaks. The widths were found to be similar indicating that the in-plane magnetic coherence is limited by the structural properties of the sample. From the (100) reflection, the basal plane structural coherence is found to be ≈450 Å for the Ho_{20}/Pr_{20} sample.

The scattering was also studied as a function of temperature, and the variation of the spiral wavevector, q, and the integrated intensity of the $(0\,0\,2-q)$ peak are shown for the Ho_{20}/Pr_{20} sample in figure 3. At a Néel temperature of 112.5 K, the wavevector is 0.271c*, which reduces on cooling until a lock-in to 0.230c* occurs at 30 K. Comparing this to the bulk variation, shown by the solid line in figure 3(a), the wavevector is larger than for the bulk at all temperatures below 110 K, which may possibly be related to the strain imposed by the lattice mismatch of Ho and Pr [18]. The intensity of the peak follows a simple Brillouin function, and similar results were obtained for the other samples.

The only other study of light-rare-earth superlattices has been of Nd/Y [4], in which the magnetic light-rare-earth blocks were separated by the non-magnetic Y layers. As with the Ho/Pr superlattices, the magnetic coherence length was limited to the thickness of a single Nd block. This occurred for most samples except that if the Y blocks became very thin (8–10 atomic planes) the coherence length was somewhat larger, possibly because of alloying and surface roughness.

There are two superlattice systems composed of a heavy rare earth and a non-magnetic

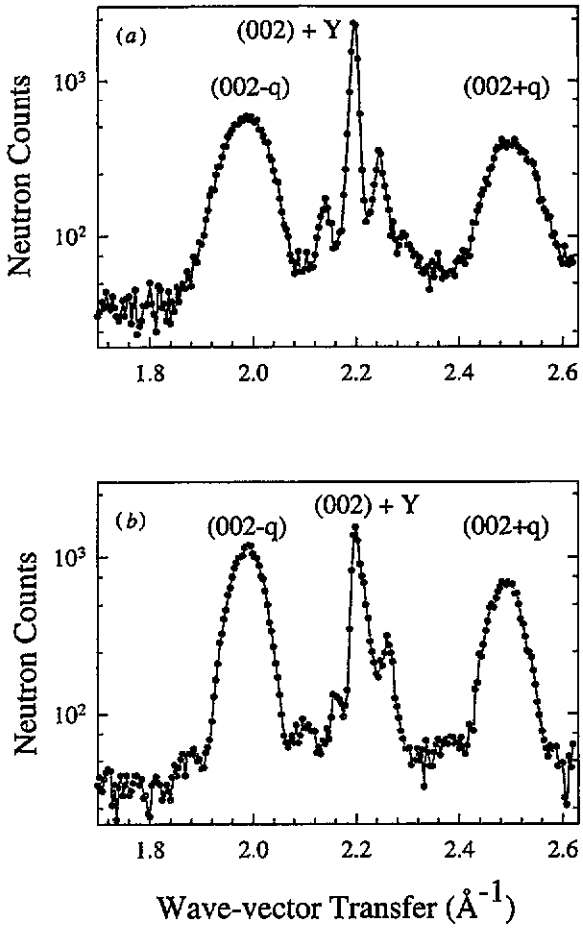

Figure 2. The neutron scattering observed at 10 K with the wavevector transfer along $[00\ell]$ for (a) the Ho_{20}/Pr_{20} sample and (b) Ho_{30}/Pr_{10}. Broad magnetic peaks occur at q from nuclear peaks and indicate helical magnetic ordering in Ho blocks, which does not have long-range coherence along c.

spacer that have also been reported not to develop long-range magnetic order across the spacer layer. Dy/Sc [19] superlattices grown in a similar way to the Dy/Y samples [2], i.e. with the basal planes perpendicular to the growth direction, display short-range order in the absence of an externally applied magnetic field. However, the measurements are complicated by the ferromagnetic structure within each Dy block and the large lattice mismatch between Dy and Sc. This result is nevertheless surprising, as calculations suggest that Sc should have a conduction electron susceptibility along the c axis [22] that is very similar to that of Y and the heavy rare earths [21], and so further investigations of superlattices containing Sc would be helpful in clarifying this situation. The other system is Dy/Y grown with the b axis as the growth direction [20]. In this case there is no long-range order, and the authors suggest that this is because the exchange function, $\mathcal{J}(\boldsymbol{R})$, in Y is long ranged along the c axis, but only very short ranged along the b axis.

We consider that there are two distinct explanations for the lack of long-range magnetic order in the Ho/Pr superlattices. The first approach would attribute the lack of coherence to

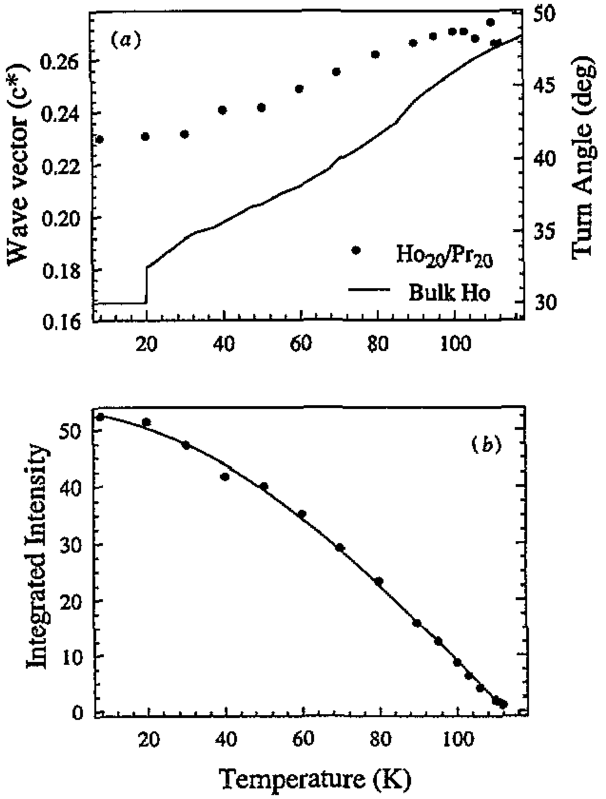

Figure 3. (a) The variation of the spiral wavevector, q, with temperature for the Ho_{20}/Pr_{20} sample. This is larger than the bulk value for Ho (solid line). (b) The integrated intensity of the $(0\,0\,2-q)$ peak for this sample reduces on warming following a simple Brillouin function. This indicates $T_N \approx 112.5$ K.

the fact that $\mathcal{J}(\boldsymbol{R})$ along the c axis is of much shorter range than for Y or Lu spacer layers. Unfortunately, at present the conduction electron susceptibility of Pr along the c axis is not well known, because calculations by Liu *et al* [21] give a larger susceptibility than in Ho, and one that would favour a ferromagnetic alignment of Pr moments in successive basal planes along c. Experiments show that an antiferromagnetic structure occurs [15]. However, an indication that $\mathcal{J}(\boldsymbol{R})$ along c extends beyond nearest neighbours is the fact the magnetic excitons show a significant dispersion along this direction [15]. The alternative approach, as discussed elsewhere [23], is to consider that the long-range interaction observed in superlattices comprised of a magnetic heavy rare earth with Y or Lu can be more reasonably understood by the development of a coherent band structure for the whole superlattice, as the two elements have very similar Fermi surfaces. In contrast, Ho and Pr have very different Fermi surfaces [15], and this causes the electrons at the Fermi surface to be confined to either Pr or Ho blocks. These are then unable to propagate a long-range coherent magnetic structure.

In conclusion, we have studied the crystallographic and magnetic properties of three Ho/Pr superlattices. The two elements retain their bulklike structures, namely hcp for Ho and dhcp for Pr, but the stacking sequence of hexagonal layers is not coherent along the growth direction. Below the Néel temperature of ~115 K, the Ho moments form a helical structure in which the magnetic order is coherent over only one Ho block. The lack of magnetic coherence along the c axis may be due to the difference in the band structures of the two elements.

We would like to acknowledge Allan Mackintosh for many useful discussions. Financial support for the work at Risø was provided by the EU under the Large Scale Facility Programme, and the work in Oxford was funded by the EPSRC.

References

[1] Majkrzak C F, Kwo J, Hong M, Yafet Y, Doon Gibbs, Chien C L and Bohr J 1991 *Advances in Physics* **40** 99
[2] Erwin R W, Rhyne J J, Salamon M B, Borchers J, Sinha S, Du R, Cunningham J E and Flynn C P 1987 *Phys. Rev. B* **35** 6808
[3] Swaddling P P, McMorrow D F, Simpson J A, Wells M R, Ward R C C and Clausen K N 1993 *J. Phys.: Condensed Matter* **5** L481
[4] Everitt B A, Borchers J A, Salamon M B, Rhyne J J, Erwin R W, Park B J and Flynn C P 1995 *J. Magn. Magn. Mater.* **140–144** 769
[5] Koehler W C, Cable J W, Wilkinson M K and Wollan F O 1966 *Phys. Rev.* **151** 414
[6] Gibbs D, Moncton D E, D'Amico K L, Bohr J and Grier B H 1985 *Phys. Rev. Lett.* **55** 234
[7] Cowley R A and Bates S 1988 *J. Phys. C.: Solid State Phys.* **21** 4113
[8] Bates S, Patterson C, McIntyre G J, Palmer S B, Mayer A, Cowley R A and Melville R 1988 *J. Phys. C.: Solid State Phys.* **21** 4125
[9] Lea K R, Leask M J M and Wolf W P 1962 *J. Phys. Chem. Solids* **23** 1381
[10] Jensen J 1976 *J. Phys. C.:Solid State Phys.* **9** 111
[11] Bleaney B 1972 1972 *Magnetic Properties of Rare Earth Metals* ed R J Elliott (London: Plenum) p 383
[12] McCausland M A H and Mackenzie I S 1979 *Adv. Phys.* **28** 305
[13] McEwen K A and Stirling W G 1981 *J. Phys. C.: Solid State Phys.* **14** 157
[14] H. Bjerrum Møller, Jensen J Z, Wulff M, Mackintosh A R, McMasters O D and Geschneider K A Jr 1982 *Phys. Rev. Lett.* **49** 482
[15] Jensen J and Mackintosh A R 1989 *Rare Earth Magnetism—Structures and Excitations* (Oxford: Oxford University Press)
[16] McMorrow D F, Jehan D A, Swaddling P P, Cowley R A, Ward R C C, Wells M R and Clausen K N 1993 *Physica* B **192** 150
[17] Flynn C P 1988 *J. Phys. F.: Met. Phys.* **18** L195
[18] Jehan D A, McMorrow D F, Cowley R A, Wells M R, Ward R C C, Hagman N and Clausen K N 1993 *Phys. Rev.* B **48** 5594
[19] Tsui F, Flynn C P, Beach R S, Borchers J A, Erwin R W and Rhyne J J 1993 *J. Appl. Phys.* **73** 6904
[20] Flynn C P, Tsui F, Salamon M B, Erwin R W and Rhyne J J 1989 *J. Phys.: Condens. Matt.* **1** 5997
[21] Liu S H, Gupta R P and Sinha S K 1971 *Phys. Rev.* B **4** 1100
[22] Rath J and Freeman A J 1975 *Phys. Rev.* B **11** 2109
[23] Simpson J A, McMorrow D F, Cowley R A, Jehan D A, Wells M R, Ward R C C and Clausen K N 1994 *Phys. Rev. Lett.* **73** 1162